

Performance Evaluation of a Specialised Pressure Sensor for Pick and Place Operations [†]

Marut Deo Sharma ^{1,*}, Juwesh Binong ²¹ Department of Electronics and Communication Engg., North Eastern Hill University, Shillong, Shillong 793022, India; jbinong@nehu.ac.in

* Correspondence: marut.devsharma@mwu.edu.et; Tel.: +91-9411491786

[†] Presented at the 10th International Electronic Conference on Sensors and Applications (ECSA-10), 15–11 30 November 2023; Available online: <https://ecsa-10.sciforum.net/>.

Abstract: A piezo resistive electrical bagging material with minimal cost and profile, linqstat or Velostat is a good choice for pressure sensing systems in robotic arm grippers. This paper's main objective is to examine the performance of a unique Velostat-based pressure sensor system for supplying real-time grasping pressure profiles during the lifting of calibrated weights. The copper conductive tape was used to build the sensor, and it was positioned on top of and beneath the velostat sheet to serve as electrodes. The accuracy, repeatability, and hysteresis responses of the pressure sensor system were examined through a variety of experiments, as well as through testing with calibrated weights ranging from 100 gm to 2000 gm in steps. The sensor's hysteresis and nonlinear characteristics were discovered through experimental results of loading cycle measurements. The velostat proved to be a realistic option as sensitive material for sensors with a single electrode pair, depending on the sensor's sensitivity, hysteresis, reaction time, loading conditions and deformation. The area where the velostat sensor might be implemented has been verified by experimental results.

Keywords: pressure sensor; Arduino board; Velostat; calibrated weights; hysteresis; grippers; wearable sensors

1. Introduction

In research using the haptic approach and robotics applications utilizing wearable technology, force distribution sensors and contact pressure sensors are frequently used. As a result, it is crucial to thoroughly research the design and characterization of these sensors in order to produce accurate results. Three distinct physical phenomena occurring in various materials—the piezo resistive effect, piezoelectric effect, and variable capacitance—provide the three most popular approaches for designing electronic sensors for measuring force and pressure [1–3]. In numerous sorts of sensing applications, the three phenomenon have been thoroughly researched. The piezoresistive materials, however, among these three categories of physical phenomenon, enable a better metrical pressure distribution monitoring in biomedical applications due to their affordability and deterministic behavior [4].

Electrical resistance of piezo resistive materials varies in response to a deformation, by an applied force [5,6] and have an inversely proportional relationship [7]. When no force is applied, the material's electrical resistance is somewhere between mega ohms and Kilo ohms or less [8]. In this paper piezo resistive sensor was tested in response to load, hysteresis, and temporal drift tests.

Citation: Sharma, M.D.; Binong, J. Performance Evaluation of a Specialised Pressure Sensor for Pick and Place Operations. *2023*, *5*, x. <https://doi.org/10.3390/xxxxx>

Academic Editor(s):

Received: date

Revised: date

Accepted: date

Published: 15 November 2023



Copyright: © 2023 by the authors. Submitted for possible open access publication under the terms and conditions of the Creative Commons Attribution (CC BY) license (<https://creativecommons.org/licenses/by/4.0/>).

2. Materials and Methods

2.1. Sensor Fabrication

The materials needed for sensor fabrication are velostat sheet, adhesive copper tape, silver conductive fabric, silicone foam layer etc. The velostat sheet is sandwiched in between two copper conductive tapes and then silver conductive fabric is also placed covering the copper conducting tape. Over the conductive tape, a layer of silicone foam is placed so that applied pressure or force is uniformly distributed over entire surface area of sensor strip [14,15] The piezo-resistive Velostat core of the sensor has a Length of 5 mm breadth of and a thickness of 0.06 mm. The main goal of the sensor design, is to reduce the size and cost of customized sensor. Velostat is the core material of the sensor has a length of 105 mm, breadth of 65 mm and a thickness of 0.06 mm. Due to the micro-Brownian motion of the carbon filler particles in the polymer, the material’s resistance decreases as force is applied to it [19,20].

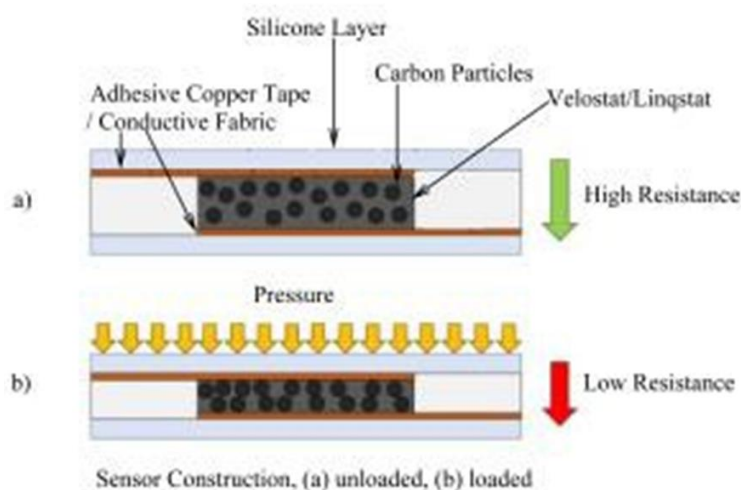


Figure 1. Sensor Construction.

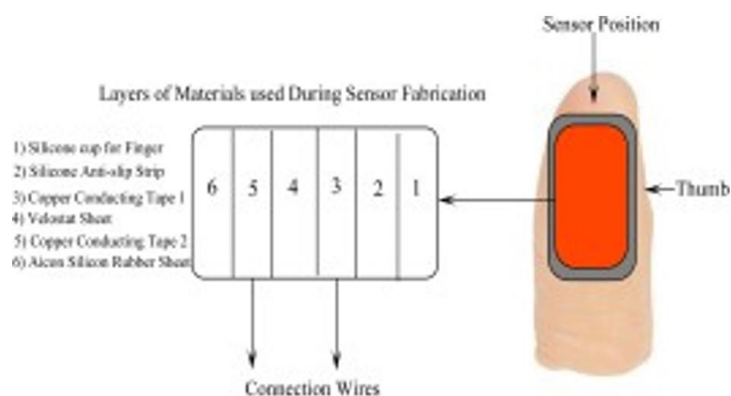


Figure 2. Layers of materials used in sensor Fabrication [18].

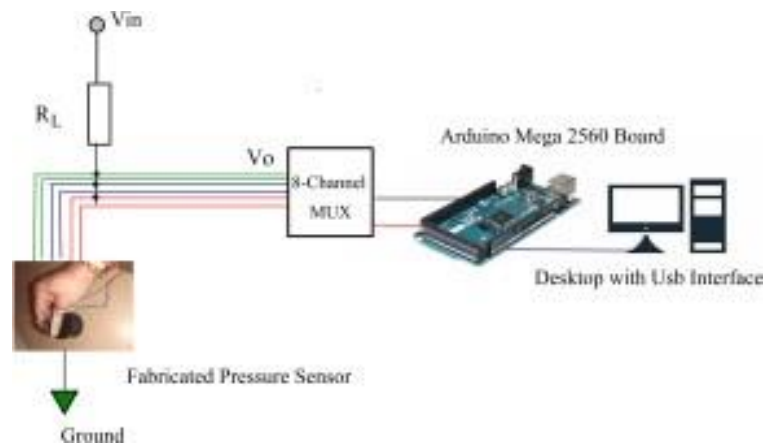


Figure 3. Experimental Setup.

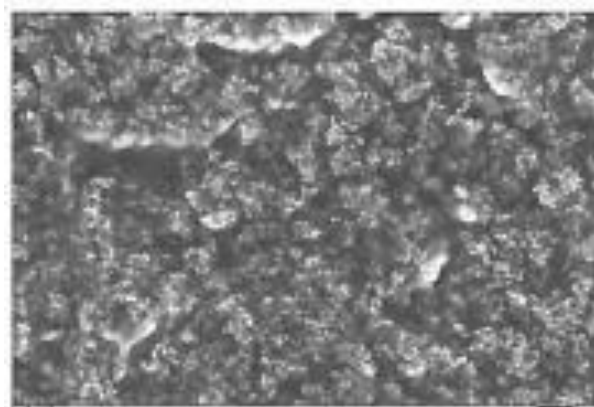


Figure 4. Electron Microscopic Image of Velostat.

2.2. Design Parameters of Conditioning Circuit

Equation (1) accurately shows the resistance-force relation for velostat [14].

$$R = \frac{\rho \times k}{F} \tag{1}$$

- R: Resistance of piezo resistive material
- k: Surface roughness factor /Coefficient
- ρ: Resistivity of the contacting surfaces
- F : Force applied normal to the contact surfaces

The effect of change in force is inversely proportional to resistance of sensor, moreover K has a direct impact on force applied while holding an object. If the value of surface is more rough greater will be the resistance and lesser force required to lift an object. As shown in Figure 4, a voltage divider circuit was used to transform the resistance of the sensors into a voltage signal by connecting them in series with a fixed resistor R (10 KΩ). Applying Ohm’s law as illustrated in Equation (2) yields the voltage read at the sensor-resistor junction.

$$V_O = V_{in} \left[\frac{\rho \times k}{F \times R_L + \rho \times k} \right] \tag{2}$$

- R_L : voltage divider circuit’s resistance
- V_{in} : sensor’s input voltage
- V_O : Voltage Divider’s output voltage

By taking into account Equations (1) and (2), the voltage force relationship is established. A Linear response might be obtained by connecting the sensor resistor between a voltage source and an input of a current to voltage converter (a virtual ground) obtaining a voltage output proportional to the piezo resistive sensor resistance [18].

2.3. Experimental Design Parameters [8–10]

The experiments focused on sensor response characteristics for distinct load levels, continuous cyclical loads, drift characteristics and variation due to loading rate changes.

2.3.1. Hysteresis

The greatest output variation between loading and unloading a single load was referred to as hysteresis.

$$\text{Hysteresis} = \frac{|V_{\text{Load}} - V_{\text{Unload}}|}{|V_{\text{Max}} - V_{\text{Min}}|} \times 100\% \quad (3)$$

where V_{Load} and V_{Unload} are the sensor voltages corresponding to the greatest difference between the loading and unloading responses, and where V_{Max} and V_{Min} are the sensor voltages at maximum and minimum load respectively [13] (Figure 6, Table 5, 6.)

2.3.2. Drift

Drift is described as a shift in sensor output over time for a specific load, typically an increase in value. With weights kept for five minutes, the sensor was loaded to 200 gm to 2000 gm in steps and the variations in resistance as well as pressure value is noted down.

2.3.3. Repeatability

The variation in output produced when a sensor is loaded to the same pressure is known as repeatability. Each sensor was loaded in the calibrated weight ranging from 100 gm to 2000 gm range (Table 8.).

2.3.4. Effect of Temperature

By heating the sensors using a hot plate or hair dryer, from room temperature up to 60°C in a step of 5 degree, At these temperatures, the sensor response was recorded for roughly 30 min with no loads and loads ranging from 200 gm to 2000 gm [11,12] (Figure 7, Table 7)

2.4. Experimental Methods

2.4.1. Pre-Commissioning Test

The fabricated sensor has to undergo various pre-commissioning test which includes, twisting effect, bending effect, stretching effect. (Table 1–4) (Figure 8–12)

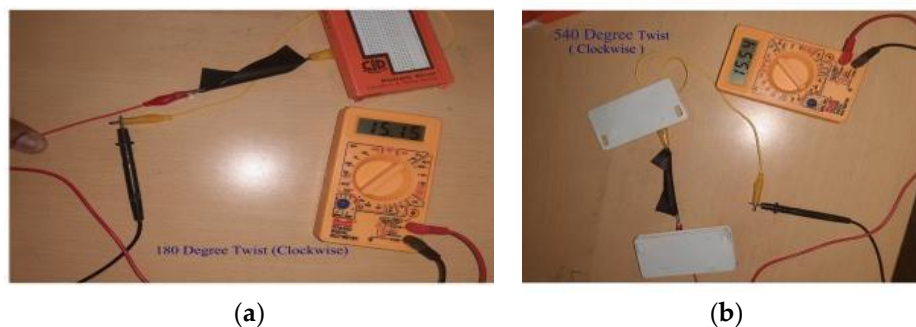


Figure 5. (a) 180° twisting of velostat strip (Clockwise); (b) 540° twisting of velostat strip (Clockwise).

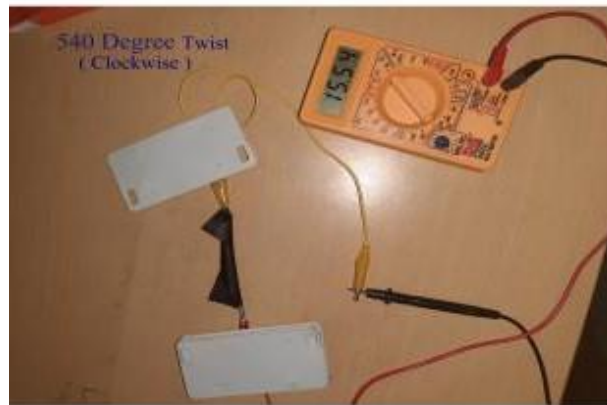


Figure 6. Loading test by calibrated weights.

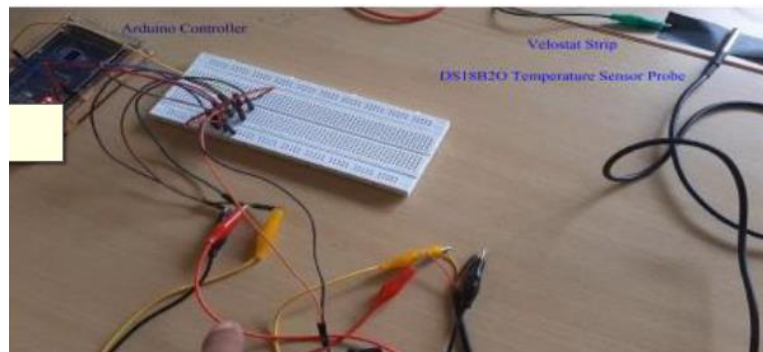


Figure 7. Temperature Test.

2.4.2. Pre and Post Commissioning Test

Table 1. Variation of velostat resistance (clockwise).

S. No	Twisting Angle (Clockwise)	Rvelostat (KΩ)	% Change in Resistance (Δ Rvelostat / Rvelostat) $\times 100\%$
1	0 ⁰ Twist (Flat Surface)	14.70 -14.81	0.673%
2	180 ⁰ Twist	15.15	2.292%
3	360 ⁰ Twist	15.40	1.655%
4	540 ⁰ Twist	15.56	1.039%

Table 2. Variation of velostat resistance (Anti-Clockwise).

S. No	Twisting Angle (Anti Clockwise)	Rvelostat (KΩ)	% Change in Resistance (Δ Rvelostat / Rvelostat) $\times 100\%$
1	0 ⁰ Twist (Flat Surface)	14.77–14.80	0.673%
2	180 ⁰ Twist	15.13	2.292%
3	360 ⁰ Twist	15.32	1.655%
4	540 ⁰ Twist	15.50	1.039%

Table 3. Bending Test on velostat Strip.

S. No	Bend Angle (Degree)	Rvelostat (K Ω)	% Change in Velostat Resistance (Δ Rvelostat / Rvelostat) \times 100%
1	0 ⁰ (Flat Surface)	14.70	0.673%
2	30 ⁰ (Light Bend)	14.82	2.297%
3	45 ⁰ (Moderate bend)	14.90	1.256%
4	90 ⁰ (Omega Bend)	15.56	1.173%
5	Pinch Bend	13.05	-16.124%

Table 4. Stretching Test on velostat Strip.

S. No	Velostat Strip Length (L+ δ L)cm	Rvelostat (K Ω)	% Change in Velostat Resistance (Δ Rvelostat / Rvelostat) \times 100%
1	No Stretch (10.5)	14.55–14.68	0.855%
2	Light Stretch (10.55)	15.60	6.768%
3	Med. Stretch (10.6)	15.90	1.923%
4	High Stretch (10.7)	15.73	1.173%
5	Pinch Bend	13.05	-16.124%

Table 5. Loading Test on sensor (Ascending weights).

S. No	Calibrated Weights (Grams)	Resistance Range Rvelostat (K Ω)	% Change in Resistance (Δ Rvelostat / Rvelostat) 100%
1	0	17.1–18.2	-30%
2	250	12.23–12.60	-11.90%
3	500	10.99–11.10	-0.09%
4	750	10.85–10.93	-4.55%
5	1000	10.15–10.50	-12.38%
6	1250	9.11–9.20	-2.17%
7	1500	8.94–9.00	-0.89%
8	1750	8.67–8.92	-4.71%
9	2000	8.45–8.50	0%

Table 6. Loading Test on sensor (Descending weights).

S. No	Calibrated Weights (Grams)	Resistance Range Rvelostat (K Ω)	% Change in Resistance (Δ Rvelostat / Rvelostat) 100%
1	2000	8.63–8.69	0%
2	1750	8.85–8.92	2.55%
3	1500	9.10–9.17	2.83%
4	1250	9.23–9.57	1.43%
5	1000	10.60–10.85	14.84%
6	750	11.03–11.86	4.06%
7	500	13.50–13.84	22.40%
8	250	14.00–15.56	3.70%
9	0	16.44–17.54	25.29%

Table 7. Effect of temperature on velostat material.

S. No	Ambience Temperature(0C)	R _{velostat} (KΩ)	% Change in Resistance (Δ R _{velostat} / R _{velostat}) 100%
1	24.44 ⁰ C (Room Temp.)	13.1	0%
2	27 ⁰ C	14.2	8.40%
3	32 ⁰ C	14.7	3.52%
4	37 ⁰ C	15.3	3.92%
5	42 ⁰ C	18.7	22.22%
6	47 ⁰ C	21.9	17.10%
7	52 ⁰ C	26.1	19.18%
8	57 ⁰ C	20.4	-21.83%
9	62 ⁰ C	18.5	-9.31%

Table 8. Hysteresis and Drift test on sensor by calibrated weights.

S. No	Calibrated Weights (Grams)	Hysteresis	Voltage Drift	
			Δ V0	Δ R _{velostat} (Ω)
1	0	0%	0	0
2	250	-1.408451%	0.47	58002.11
3	500	12.67606%	0.09	4705.14
4	750	1.408451%	0.12	5565.36
5	1000	21.121761%	0.08	4154.8
6	1250	-14.08451%	0.14	5512.6
7	1500	-42.25352%	0.06	2733.62

2.4.3. Graphs

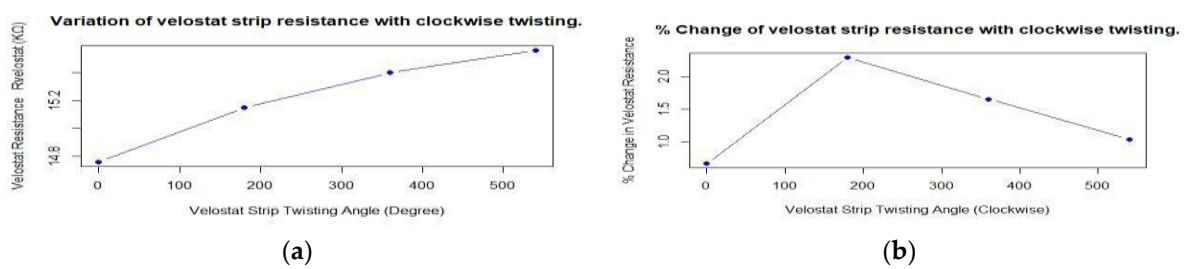


Figure 8. (a) Variation of velostat Resistance with clockwise twisting; (b) % Change of velostat resistance with clockwise twisting.

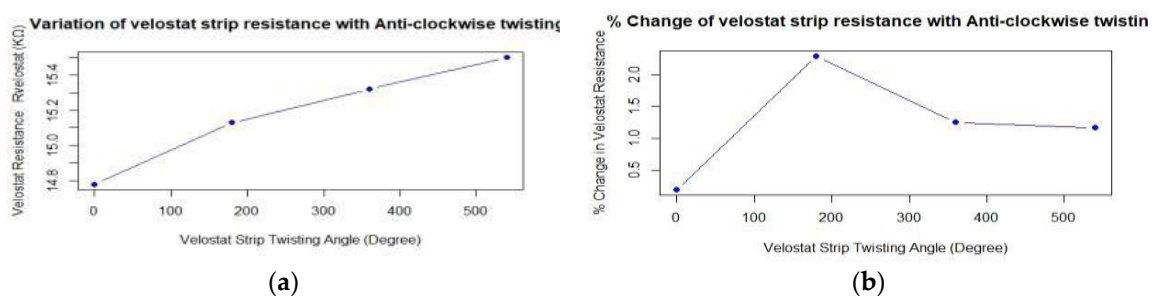


Figure 9. (a) Variation of velostat Resistance; (b) % Change of resistance with anti-clockwise twisting.

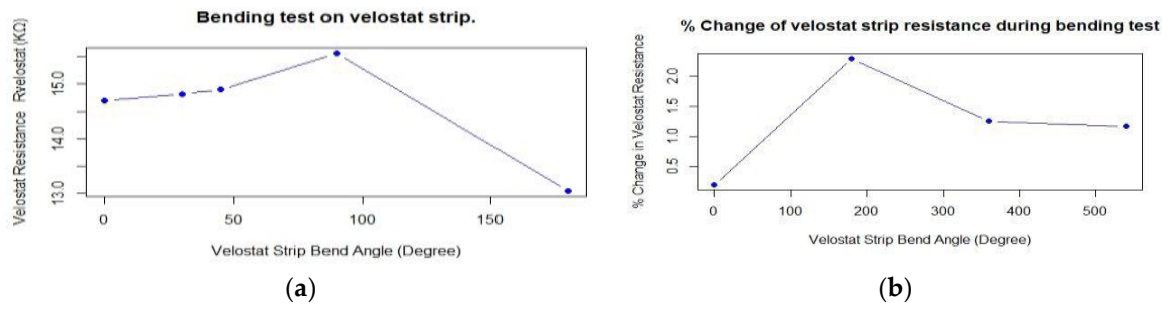


Figure 10. (a) Resistance variation in bending test; (b) % Change of resistance in bending.

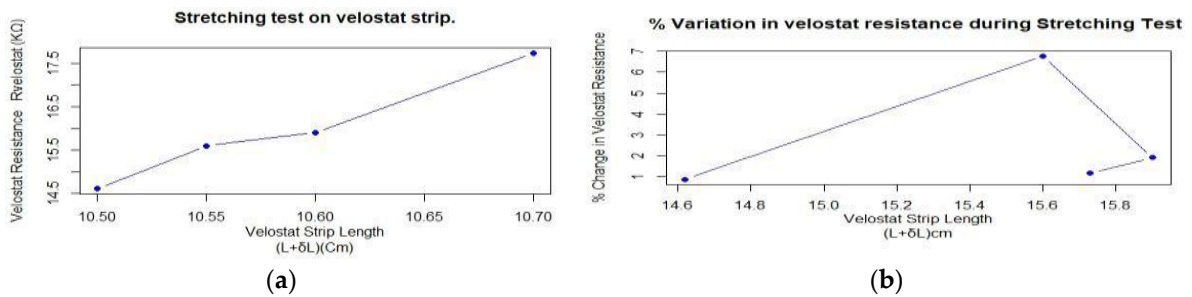


Figure 11. (a) Variation of velostat resistance with stretching test; (b) % Change of velostat resistance during stretching test.

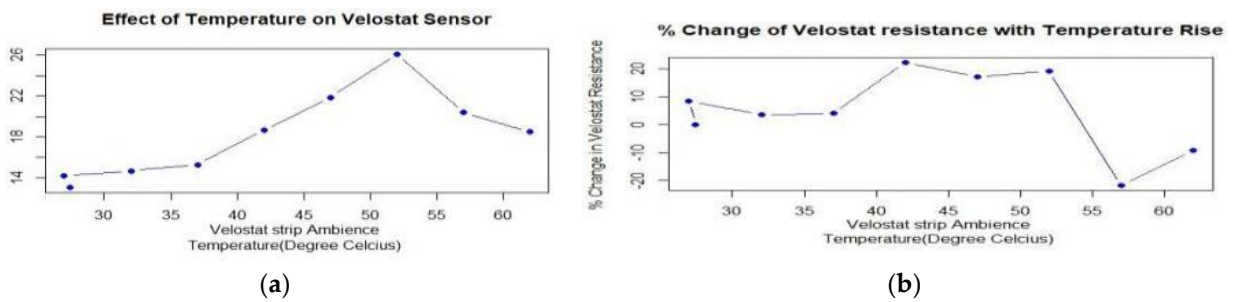


Figure 12. (a) Effect of temperature on velostat sensor; (b) % Change of velostat resistance with temperature rise.

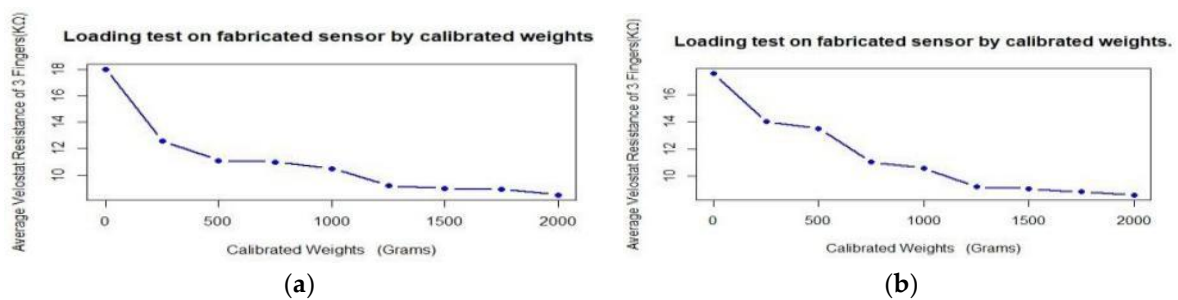


Figure 13. (a) Effect of descending weight values on sensor resistance; (b) Effect of ascending weight values on sensor resistance.

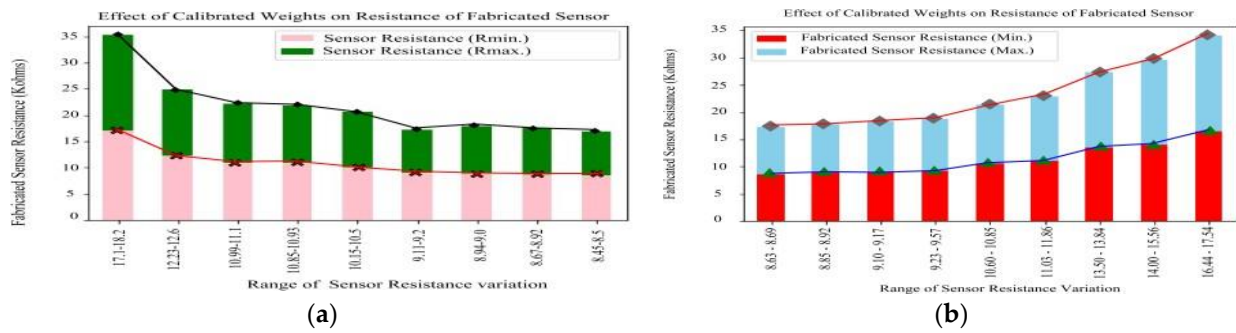


Figure 14. (a) Range of sensor resistance for descending calibrated weights; (b) Range of sensor resistance for ascending calibrated weights.

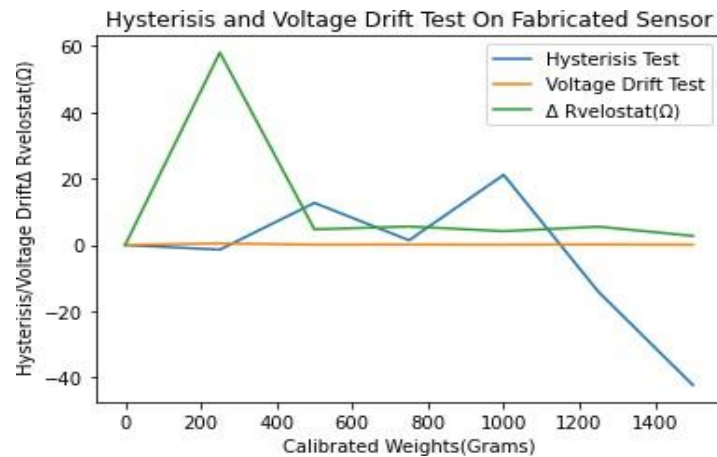


Figure 15. Performance Curve of Sensor.

Calculations

For Calibrated Weight of 1000 Grams
 Drift in Voltage = 1.10 – 1.02 = 0.08 V
 Drift in Fabricated Sensor Resistance = 39420.29 – 35245.29 = 4154.80Ω

$$Hysteresis = \frac{|1.10 - 0.95|}{|1.50 - 0.79|} \times 100 \% = 21.121761\%$$

For Calibrated Weight of 250 Grams Drift in Voltage = 0.91 – 0.44 = 0.47 V
 Drift in Fabricated Sensor Resistance = 102417 – 44414.89 = 58002.11Ω

$$Hysteresis = \frac{|0.42 - 0.79|}{|1.50 - 0.79|} \times 100 \% = -1.408451\%$$

3. Results and Discussion

In fabricated sensor, hysteresis errors were observed in the range of 21.121% to – 42.253% for ascending and descending weights shown in table.8. The sensor sensitivity changes swiftly beyond load 1000 gm, as variations in resistance is significant, opt for range of readings and then find optimal values (Figure 15a,b). The voltage drift is also quantized in sensor ranging from 0.06 V to 0.47 V shown in table.8. The effectiveness of sensor is greatly affected as temperature increases above 60°C as shown in table.7. After 55° C, the resistance of sensor drops significantly as shown in Figure 16. The significance of the sensor fabrication is that it provides sensing solutions spanning consumer, industrial, and biomedical applications, since many different engineering principles and physics phenomena are employed to sense pressure. The advantage of using velostat as pressure sensing element is of low cost, power consumption, simple electronic circuitry. The limitations associated with its high sensitivity to pressure variations, output from sensor is temperature dependent and problem with coating material and adhesives at temperature

beyond its permissible values, hysteresis can affect performance matrices like accuracy, stability, precision etc.

4. Conclusions

It is evident from the above observations and performance curves that the proposed specialized pressure sensor is working satisfactorily during pick and place operation of calibrated weights and can safely be deployed with robotic arm gripper for grasping objects.

Supplementary Materials: The following supporting information can be downloaded at: [marutdevsharma/performance-evaluation-of-especialized-Pressure-Sensor-](https://github.com/marutdevsharma/performance-evaluation-of-especialized-Pressure-Sensor-) (github.com).

Author Contributions: The following are the contributions of main and co author in this manuscript. “Conceptualization, Marut Deo Sharma ; methodology, Marut Deo Sharma; software, Marut Deo Sharma; validation, Dr Juwesh Binong ; formal analysis, Marut Deo Sharma; investigation, Marut Deo Sharma; resources, Marut Deo Sharma; data curation, Marut Deo Sharma, writing—original draft preparation, Marut Deo Sharma.; writing—review end editing, Marut Deo Sharma. All authors have read and agreed to the published version of the manuscript.

Funding: This research received no external funding.

Informed Consent Statement: Not applicable.

Data Availability Statement: The data that support the findings of this research will be available at [<https://github.com/marutdevsharma?tab=repositories>] or at DOI.

Acknowledgments: This research would not have been possible without the exceptional support of my Ph.D. supervisor and co-author Juwesh Binong. He also looked over my transcriptions and numerous questions about the sensor system design and its implementations.

Conflicts of Interest: The authors declare no conflict of interest.

References

1. Tao, L. Q., Zhang, K. N., Tian, H., Liu, Y., Wang, D. Y., Chen, Y. Q., ... & Ren, T. L. (2017). Graphene-paper pressure sensor for detecting human motions. *ACS nano*, 11(9), 8790-8795.
2. Ruth, S. R. A., Feig, V. R., Tran, H., & Bao, Z. (2020). Micro engineering pressure sensor active layers for improved performance. *Advanced Functional Materials*, 30(39), 2003491.
3. Li, J., Bao, R., Tao, J., Peng, Y., & Pan, C. (2018). Recent progress in flexible pressure sensor arrays: From design to applications. *Journal of Materials Chemistry C*, 6(44), 11878-11892.
4. Li, R., Zhou, Q., Bi, Y., Cao, S., Xia, X., Yang, A., ... & Xiao, X. (2021). Research progress of flexible capacitive pressure sensor for sensitivity enhancement approaches. *Sensors and Actuators A: Physical*, 321, 112425.
5. Luo, Z. P., Berglund, L. J., & An, K. N. (1998). Validation of F-Scan pressure sensor system: a technical note. *Journal of rehabilitation research and development*, 35, 186-186.
6. Patra, J. C., Kot, A. C., & Panda, G. (2000). An intelligent pressure sensor using neural networks. *IEEE transactions on instrumentation and measurement*, 49(4), 829-834.
7. Shirinov, A. V., & Schomburg, W. K. (2008). Pressure sensor from a PVDF film. *Sensors and Actuators A: Physical*, 142(1), 48-55.
8. Hopkins, M., Vaidyanathan, R., & McGregor, A. H. (2020). Examination of the performance characteristics of velostat as an in-socket pressure sensor. *IEEE Sensors Journal*, 20(13), 6992-7000.
9. Sergio, M., Manaresi, N., Tartagni, M., Guerrieri, R., & Canegallo, R. (2002, June). A textile based capacitive pressure sensor. In *SENSORS, 2002 IEEE* (Vol. 2, pp. 1625-1630). IEEE.
10. Boutry, C. M., Nguyen, A., Lawal, Q. O., Chortos, A., Rondeau-Gagné, S., & Bao, Z. (2015). A sensitive and biodegradable pressure sensor array for cardiovascular monitoring. *Advanced Materials*, 27(43), 6954-6961.
11. Li, Y., Samad, Y. A., & Liao, K. (2015). From cotton to wearable pressure sensor. *Journal of Materials Chemistry A*, 3(5), 2181-2187.
12. Meyer, J., Lukowicz, P., & Troster, G. (2006, October). Textile pressure sensor for muscle activity and motion detection. In *2006 10th IEEE International Symposium on Wearable Computers* (pp. 69-72). IEEE.
13. Chen, D., Cai, Y., & Huang, M. C. (2018). Customizable pressure sensor array: Design and evaluation. *IEEE Sensors Journal*, 18(15), 6337-6344.
14. Zang, Y., Zhang, F., Di, C. A., & Zhu, D. (2015). Advances of flexible pressure sensors toward artificial intelligence and health care applications. *Materials Horizons*, 2(2), 140-156.
15. Ashruf, C. M. A. (2002). Thin flexible pressure sensors. *Sensor Review*.

16. Gála, M., Barabáš, J., & Kopásková, M. (2020, September). User presence monitoring based on Velostat pressure sensors and Arduino platform. In *2020 IEEE 21st International Conference on Computational Problems of Electrical Engineering (CPEE)* (pp. 1-3). IEEE.
17. Salibindla, S., Ripoche, B., Lai, D. T., & Maas, S. (2013, April). Characterization of a new flexible pressure sensor for body sensor networks. In *2013 IEEE eighth international conference on intelligent sensors, sensor networks and information processing* (pp. 27-31). IEEE.
18. Fatema, A., Poondla, S., Mishra, R. B., & Hussain, A. M. (2021). A low-cost pressure sensor matrix for activity monitoring in stroke patients using artificial intelligence. *IEEE Sensors Journal*, *21*(7), 9546-9552.
19. Vehc, I., & Livovsky, L. (2020, May). Flexible resistive sensor based on velostat. In *2020 43rd International Spring Seminar on Electronics Technology (ISSE)* (pp. 1-6). IEEE.
20. Giovanelli, D., & Farella, E. (2016). Force sensing resistor and evaluation of technology for wearable body pressure sensing. *Journal of Sensors*, 2016.